Anisotropic Propagation of Ca^{2+} Waves in Isolated Cardiomyocytes

Jutta Engel, Martin Fechner, Andrew J. Sowerby, Simon A. E. Finch, and Anton Stier
Max Planck Institute for Biophysical Chemistry, Department of Spectroscopy, 37018 Göttingen, Germany

ABSTRACT Digital imaging microscopy of fluo-3 fluorescence was used to study the propagation of intracellular Ca^{2+} waves in isolated adult rat cardiomyocytes from 17 to 37°C. Ca^{2+} waves spread in both transverse and longitudinal direction of a myocyte. Transverse propagation was pronounced in waves starting from a focus at the edge of a myocyte and in waves following an irregular, curved path (spiral waves). For the former type of waves, propagation velocities were determined. Both transverse and longitudinal wave components propagated at constant velocity ranging from 30 to 125 μm/s. Myocytes were anisotropic with respect to wave propagation: waves propagated faster in the longitudinal than in the transverse direction. The ratio between longitudinal and transverse velocity increased from 1.30 at 17°C to 1.55 at 37°C. Apparent activation energies for transverse and longitudinal wave propagation were estimated to be −20 kJ/mol, suggesting that these processes are limited by diffusion of Ca^{2+}. Direction-dependent propagation velocities are interpreted to result from the highly ordered structure of the myocytes, especially from the anisotropic arrangement of diffusion obstacles such as myofilaments and mitochondria.

INTRODUCTION

Isolated cardiomyocytes exhibit spontaneous contractile activity that appears as a contraction band that propagates from one end of the cell to the other (Rieser et al., 1979). Using fluorescence imaging techniques and the newly developed fluorescent Ca^{2+} indicators such as indo-1, fura-2, or fluo-3, it has been found that contractile waves are preceded by propagating zones of elevated intracellular free Ca^{2+} concentration ($[Ca^{2+}]_i$), so called Ca^{2+} waves (Berlin et al., 1988; Stern et al., 1988; Takamatsu and Wier, 1990; Ishide et al., 1990; Grouselle et al., 1991; Williams et al., 1992). Ca^{2+} waves are favored under conditions of increased $[Ca^{2+}]_i$ load (Stern et al., 1988; Takamatsu and Wier, 1990; Grouselle et al., 1991). Although it is unclear at present whether Ca^{2+} waves occur in the intact heart, they may have relevance to pathological phenomena such as aftercontractions, arrhythmia, and depression of systolic and diastolic function (Stern et al., 1988; Lakatta, 1992; Fabiato, 1992).

The mechanisms underlying the initiation and propagation of a Ca^{2+} wave have not been clearly resolved (Wier and Blatter 1991; Stern, 1992; Fabiato, 1992). Ca^{2+} waves are assumed to spread by regenerative Ca^{2+}-induced Ca^{2+} release (CICR; Fabiato, 1985) from the sarcoplasmic reticulum (SR). CICR is part of physiological excitation-contraction coupling where it mediates a large amplification of Ca^{2+} that flows in through voltage-activated Ca^{2+} channels during depolarization of the cell (Fleischer and Inui, 1989). This leads to a synchronous elevation in $[Ca^{2+}]_i$, which in turn activates the myofilaments. In a Ca^{2+} wave, however, this autocatalytic mechanism is decoupled from electrical excitation. It is assumed that locally released Ca^{2+} diffuses to adjacent release sites and induces regenerative CICR. The propagating release of constant amounts of Ca^{2+} from the SR followed by propagating re-uptake by the SR results in a Ca^{2+} wave of constant width and velocity. It becomes directed because of Ca^{2+} removal at the trailing edge and refractoriness of the SR to sustained Ca^{2+} release (Wier and Blatter, 1991; Stern, 1992; Lakatta, 1992; Fabiato, 1985, 1992).

To obtain information about the mechanisms of Ca^{2+} release, diffusion, and re-uptake, spatio-temporal properties of wave propagation have been investigated (Berlin et al., 1988; Takamatsu and Wier, 1990; Ishide at al., 1990, 1992; Grouselle et al., 1991; Williams et al., 1992). It has been found that waves mostly arise at one cell end and travel at constant velocity to the opposite end where they disappear. Although it has been observed that waves arising at a focus in the cell spread in both longitudinal and transverse direction (Berlin et al., 1988; Takamatsu and Wier, 1990; Williams et al., 1992) two-dimensional wave propagation has not been systematically investigated. The aim of the present study was to characterize two-dimensional wave spreading in isolated cardiomyocytes in more detail. The fluorescent Ca^{2+} indicator fluo-3 and an imaging system with a temporal resolution of 40 ms were used to determine direction-dependent propagation velocities in the temperature range 17–37°C.

MATERIALS AND METHODS

Preparation of cells

Ventricular cardiomyocytes were isolated by using a modified Langendorff reverse perfusion method (Piper et al., 1982). The heart of an ether-anesthesized, heparinized Sprague-Dawley rat (200–300 g) was excised, and the aorta was cannulated. It was perfused in sequence with the following solutions (bubbled with 95% O_2:5% CO_2) at 37°C: (i) a modified Krebs-Henseleit (KHS) solution containing (in mM) 106 NaCl, 25 $NaHCO_3$, 4.6

Received for publication 30 November 1993 and in final form 28 February 1994.

Address reprint requests to Dr. Jutta Engel, Georg August University, Institute of Physiology, Dept. of Neurophysiology, Humboldt-Allee 23, 37073 Göttingen, FRG. Tel.: 49-551-395913; Fax: 49-551-395923; E-mail: je@helena.ukps.gwdg.de.

J. Engel's present address: Georg August University, Institute of Physiology, Dept. of Neurophysiology, Humboldtallee 23, 37073 Göttingen, Germany.

A. J. Sowerby's present adress: University of Leicester, Dept. of Biochemistry, Adrian Building, University Road, Leicester LE1 7RH, England.

0006-3495/94/06/1756/07 $2.00

KCl, 1.1 $MgSO_4$, 1.2 KH_2PO_4, 1 $CaCl_2$, 8.3 glucose, 20 taurine, 10 creatine, 5 ribose, 2 sodium pyruvate, 0.1 allopurinol, 0.01 adenine, pH 7.4, 300 mOsm, for 5 min; (ii) KHS without Ca^{2+} for 8 min; (iii) KHS without Ca^{2+} containing 0.3–0.6 mg/ml collagenase type II (Sigma, München, FRG), 0.12 mg/ml dispase (Boehringer Mannheim, FRG), 0.12 mg/ml trypsin (Serva, Heidelberg, FRG), and 1.2 mg/ml BSA (Serva) for 6–8 min. The ventricles were cut into pieces and gently shaken in KHS containing 0.04 mg/ml DNAse type IV (Sigma) and 25 μM Ca^{2+}. The cell suspension was filtered through nylon gauze and centrifuged at 10 $\times$ *g* for 5 min. The sediment was washed with DNAse solution containing 50 μM Ca^{2+}. Cells were centrifuged again and resuspended in KHS at 150 μM Ca^{2+}. After 10-min equilibration, Ca^{2+} was added to give a concentration of 500 μM. The cells were centrifuged, resuspended in 4 ml of Medium 199 (Boehringer Mannheim) supplemented with 100 units/ml penicillin/streptomycin (Gibco Europe GmbH, Karlsruhe, FRG), 0.05 mg/ml gentamicin (Gibco), 10 mM HEPES, 5% fetal calf serum (FCS, Boehringer Mannheim), 0.005 mg/ml insulin (Sigma) at a final Ca^{2+} concentration of 1 mM. They were plated into plastic dishes where they attached to glass coverslips, which had been fixed to the dish with paraffin wax and preincubated with Medium 199 and 5% FCS for 12 h. The preparation yielded 70–80% rod-shaped cardiomyocytes, most of which were Ca^{2+}-tolerant. Cells were used for experiments within 30 h.

Ca^{2+} indicator and labeling of cells

Cells were labeled with 2 μM fluo-3 acetoxymethyl (AM) ester (Molecular Probes, Eugene, OR) at 22°C for 30 min. The labeling solution was prepared by dissolving 50 μg of the dye in 15 μl of an 8% (w/w) solution of Pluronic F-127 (BASF, Wyandotte) in DMSO and diluting it slowly with 20 ml of HEPES buffer (125 mM NaCl, 2.6 mM KCl, 1.2 mM $MgSO_4$, 1 mM $CaCl_2$, 10 mM glucose, 20 mM HEPES, 1 mg/ml BSA, pH 7.4, 300 mOsm) in an ultrasound bath. Cells were washed with buffer and incubated for 1 h to allow for dye hydrolysis. The coverslip was mounted into a 20 μl perfusion chamber that was continuously perfused with HEPES buffer without serum albumin at a rate of 100 μl/min. When required, chamber and microscope stage were heated to 27 or 37°C with an air stream incubator (Zeiss, Oberkochen, FRG). Upon binding Ca^{2+}, the dye fluo-3 changes its fluorescence intensity by a factor of 40 (Minta et al., 1989). Therefore, an increase in fluorescence intensity corresponds to an increase in Ca^{2+}. Calibration of fluorescence intensities in terms of absolute Ca^{2+} concentrations is difficult for a single wavelength indicator such as fluo-3 and has not been attempted in these experiments.

Experimental setup

An inverted microscope (Zeiss Axiomat) was run in the epifluorescence mode with the 488-nm line of an argon ion laser (Series 2000, Spectra Physics, Mountain View, CA) as light source. The excitation beam was attenuated with neutral density filters, passed through a frosted glass screen, and reflected off a dichroic mirror (Zeiss) to pass through the objective lens (x100 Planapo oil, N.A. 1.3, Zeiss). It was arranged to be focused at infinity as it passed through the object plane. Emitted fluorescence passed the dichroic mirror and was detected by a low light level intensifying video camera (VIM C2400, Hamamatsu Photonics Europa GmbH, Seefeld, FRG). Images were acquired at video rate (25 Hz interlaced) and recorded with a Panasonic video recorder (Matsushita Electric Industrial Co., Osaka, Japan).

Image processing

Video frames were digitized by a frame grabber (VTE Digital Braunschweig, FRG) and transferred to a Silicon Graphics Workstation 4D/35. Processing of the images (512 $\times$ 795 pixels, 8-bit depth) was carried out with user-written routines based on the software IDL (Research Systems Inc., Boulder, CO). Each series of images displaying a Ca^{2+} wave was scaled between pixel intensity 0 (background fluorescence) and 255 (maximum fluorescence in that series). Fluorescence intensity profiles through a cell were obtained after smoothing the images using a box car averaging procedure of 11 pixels (1.9 μm) width. Contours of fluorescence intensity were evaluated after averaging images by 16x16 pixels (2.7 $\times$ 2.7 μm).

RESULTS

Only rod-shaped cells with pronounced striations were chosen for imaging. Cells of inhomogeneous thickness or with branches vertical to the field of view were avoided. At 37°C, about 20% of the myocytes showed one spontaneous Ca^{2+} wave per minute. These waves mostly started at one end of a cell and travelled to the opposite end. In most cases, a point focus of the wave could not be identified. Rather, the waves started along one end of the myocyte. Within one or two frames (40 or 80 ms), the wave front became parallel to the short axis of the cell so only longitudinal propagation (parallel to the myofilaments) could be observed with our time resolution.

Transverse wave propagation was observed in those waves that started from a focal point at an edge or a side of the cell as well as in "spiral" waves. Fig. 1 shows the two-dimensional propagation of a Ca^{2+} wave that arose at a long side of the cell. Starting from the focus the wave spread in all directions. It propagated in an elliptic manner, indicating that the velocities of the longitudinal wave fronts were larger than that of the transverse one. When the transverse wave front reached the opposite side of cell the wave broke up in two longitudinal waves, which travelled to the ends of the cell.

Transverse wave propagation was also apparent in waves that did not move linearly, but adopted a curved path (spiral wave, Fig. 2). To demonstrate the changes in propagation direction of that wave, the displacement of an arbitrarily chosen contour line of a pixel intensity of 90 above background was plotted inside the contour line of the resting cell (Fig. 2 *A*). The wave adopted a curved path with a turn at the right end indicating the existence of at least three refractory areas in which CICR must have been inhibited (Fig. 2 *B*). The reason for this inhibition is unclear. CICR may have been temporarily inhibited because of localized depletion of the SR or localized inactivation of the release mechanism which may apply to the inhibitory regions 1 and 2. Another possibility is the ultrastructural discontinuity of the SR and of the diffusional space for Ca^{2+}. The nucleus of cardiomyocytes has a size of 25 $\times$ 4 μm and is surrounded by mitochondria and other organelles. Thus, it may well act as a barrier to CICR propagation, especially in narrow or flat cells. The inhibitory zone 3 in Fig. 2 *B* may reflect the existence of a nucleus, because it is comparable to it in size and shape.

To quantify longitudinal and transverse wave propagation, cells exhibiting regular, two-dimensional wave spreading without apparent refractory zones were selected and propagation velocities were determined. Fig. 3 depicts two-dimensional propagation of a Ca^{2+} wave at 27°C and illustrates the principle of velocity determination. The wave started at the lower left cell edge and spread in all directions in an elliptic manner as shown by the propagation of an

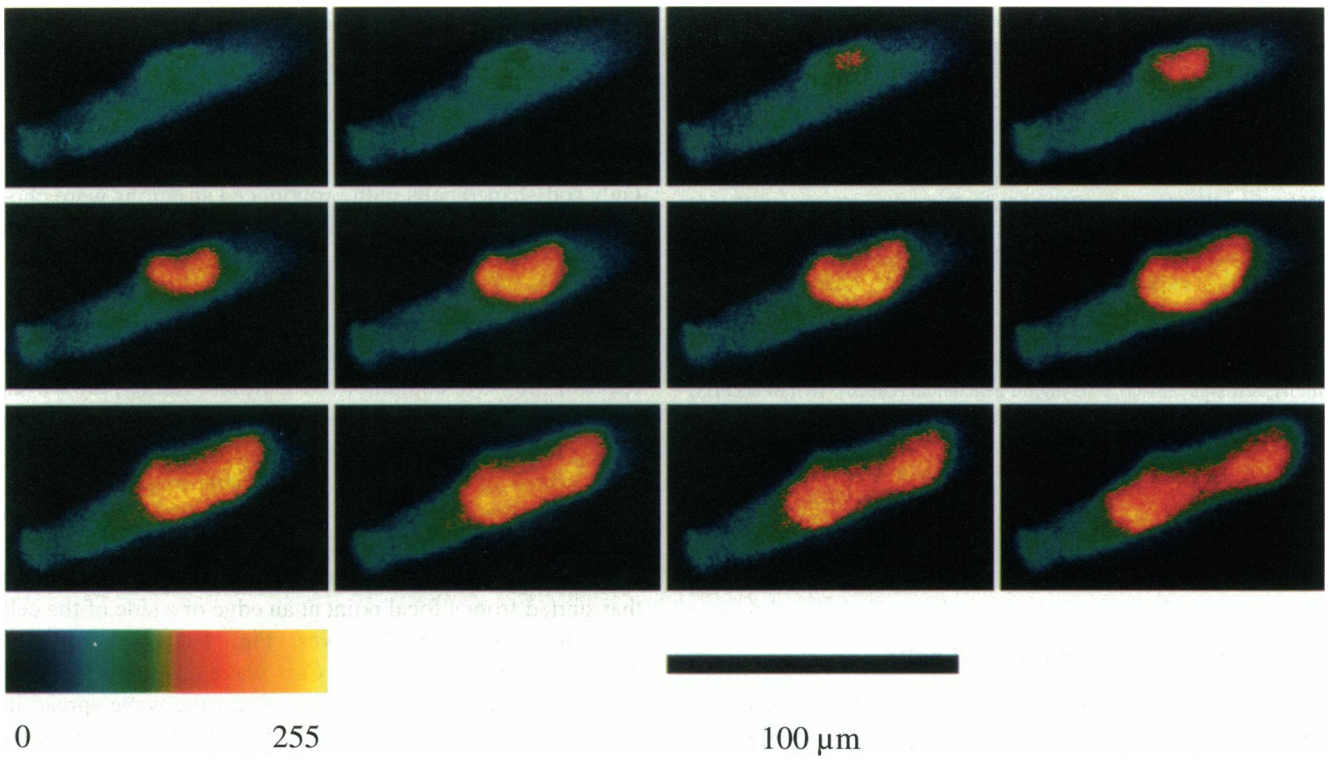

FIGURE 1 A sequence of fluorescence images displaying anisotropic spreading of a Ca^{2+} wave in a fluo-3-loaded cardiomyocyte at 37°C. Images follow one another from left to right and from top to bottom. The time interval between successive images is 40 ms. The wave arises at a lateral focus (*second image*) and spreads in all directions. Propagation is faster in the longitudinal than in the transverse direction. When the wave reaches the other side of the cell it breaks up in two longitudinal waves that travel to opposite cell ends (*last row*). Images were scaled between pixel intensity 0 (background) and 255 (maximum intensity of the series), see color bar.

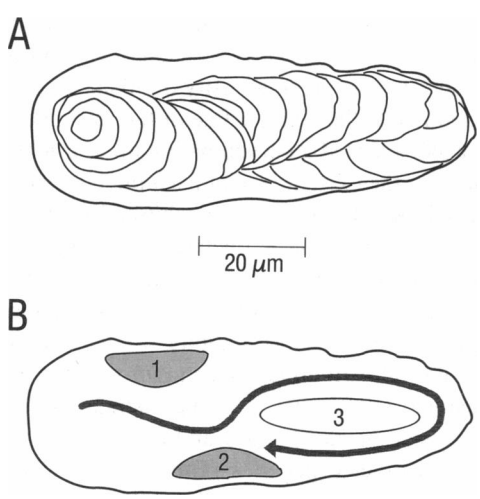

FIGURE 2 Complex pattern of Ca^{2+} wave propagation in a cardiomyocyte ("spiral" wave) with longitudinal and transverse components at 37°C. (*A*) The propagation of an arbitrary contour line of fluo-3 fluorescence (pixel intensity 90) inside the contour of the cell (pixel intensity 20) is shown. Temporal distance between contour lines is 80 ms; previous contour lines partially overlap and hide consecutive ones. (*B*) The wave takes a curved path through the cell as depicted by the arrow. This is apparently caused by the existence of refractory zones (*encircled* areas 1–3).

arbitrary contour level of pixel intensity 50 during the first 200 ms (*A*). Sections along the longitudinal and the transverse axis of the cell image as a function of time yielded the profiles of fluorescence intensity shown in B. To calculate wave velocities, the positions of the wave front were determined. As the wave front extended over 10–20 μm, we chose that x-position with the steepest slope. Because this procedure is somewhat arbitrary, it was repeated 3 times for every wave and direction, and the x-positions were averaged. Fig. 3 *C* shows the average distances travelled by the longitudinal and transversal wave components as a function of time. Both wave components propagated at constant velocity; linear regression yielded a longitudinal velocity of 79 μm/s ($r = 0.9996$) and a transverse velocity of 56 μm/s ($r = 0.9991$). In general, regression coefficients were larger than 0.98, indicating that both longitudinal and transversal wave components moved at constant velocity.

According to the procedure described, wave velocities were determined at 17, 27, and 37°C. Fig. 4 shows the mean longitudinal and transverse velocities of Ca^{2+} waves at the three temperatures. Both mean longitudinal and mean transverse velocity increased with temperature. At every temperature, mean transverse velocity was significantly smaller than the longitudinal one (Students t-test, $p = 0.05$).

For those Ca^{2+} waves in which a transverse propagation component could be determined, ratios between longitudinal (v_l) and transverse (v_t) wave velocities were calculated. At 17°C, there were 2 (out of 14) waves with v_t larger than v_l. Above 17°C, however, v_t was always found to be smaller than v_l. Table 1 shows that the mean ratio v_l/v_t increased from

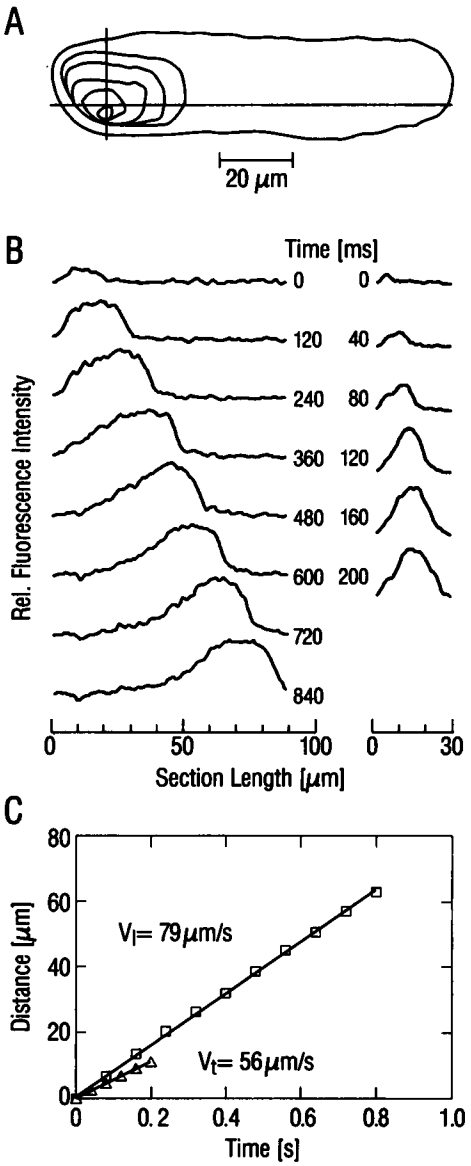

FIGURE 3 Anisotropic propagation of a Ca^{2+} wave in an isolated cardiomyocyte at 27°C measured as fluo-3 fluorescence. (*A*) Wave propagation is illustrated in terms of the propagation of an arbitrary contour line of fluo-3 fluorescence (pixel intensity 50) inside the contour of the cell (pixel intensity 20) during the first 200 ms. The wave arises at a lateral focus and spreads in an elliptic manner. Temporal distance between consecutive contour lines is 40 ms. In *B*, longitudinal (*left*) and transversal (*right*) fluorescence intensity profiles, which were determined along the sections depicted in *A*, are plotted for the times indicated. (*C*) Linear propagation of the longitudinal (□) and of the transverse wave front (△) as a function of time. Coordinates of the steepest increase of a wave front were determined in triplicate from the section plots; SDs were smaller than symbol size. Velocities were obtained by linear regression; correlation coefficients were 0.999.

1.3 at 17°C to 1.55 at 37°C. Mean ratios at 17 and 37°C differed significantly ($p = 0.05$). This confirms the findings of Figs. 1 and 3 that cardiomyocytes are anisotropic with respect to Ca^{2+} wave propagation and further indicates that this anisotropy increases with temperature.

The dependence of Ca^{2+} wave velocities on temperature was analyzed in an Arrhenius plot (Fig. 5). The logarithm of

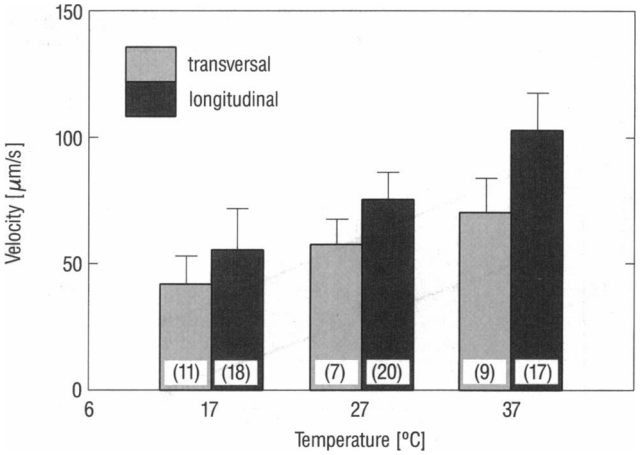

FIGURE 4 Mean longitudinal and transverse velocities of propagating Ca^{2+} waves in cardiomyocytes as a function of temperature. Wave velocities were determined following the procedure shown in Fig. 1, *B* and *C*. Light bars represent mean velocities + SD of transverse wave components, dark bars those of longitudinal wave components; the number of waves is given at the bottom of the bars. The differences between transverse and longitudinal velocities were statistically significant according to Student's t-test for $p = 0.05$ at the three temperatures examined.

TABLE 1 Anisotropy of Ca^{2+} wave propagation increases with temperature

Temperature	Ratio of velocities Longitudinal/Transversal
°C	
17	1.30 ± 0.29 (14)*
27	1.36 ± 0.29 (10)
37	1.55 ± 0.23 (9)*

Ratios between velocities of longitudinal and transverse components of individual Ca^{2+} waves were determined. Data represent mean ± SD (number of waves).
* Significant difference ($p = 0.05$).

velocities depended linearly on inverse temperature, and apparent activation energies were 23.4 kJ/mol and 19.5 kJ/mol for longitudinal and transverse wave propagation, respectively. Taking into account that there are only three data points for every curve and the size of the SD, it is reasonable to assume that the apparent activation energies for longitudinal and transversal wave propagation are equal. It remains to explain the absolute difference between v_l and v_t in the temperature range examined.

DISCUSSION

Using digital imaging microscopy of fluo-3 fluorescence, we have investigated longitudinal and transverse propagation characteristics of spontaneously occurring Ca^{2+} waves in isolated cardiomyocytes. In principle, Ca^{2+} waves spread three-dimensionally. Our measurements of fluorescence intensity projected on the object plane neglect the third dimension, i.e., wave spreading vertical to this plane. However, in view of the cylindrical symmetry of both shape and internal structure of a cardiomyocyte, transverse and vertical wave propagation should be similar.

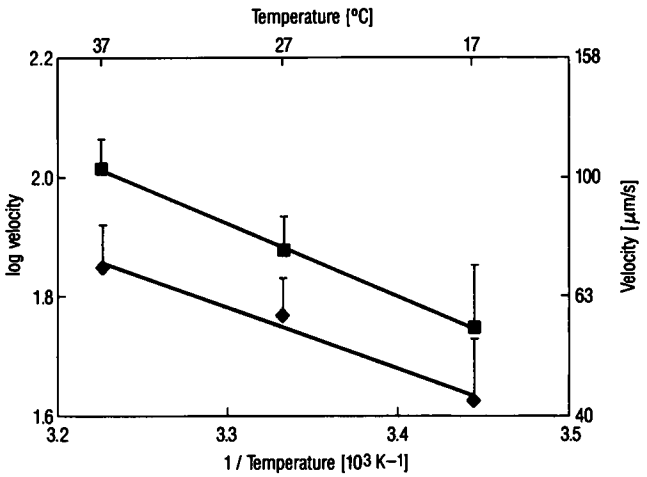

FIGURE 5 Temperature dependence of the velocity of Ca^{2+} waves expressed as an Arrhenius plot. Data for longitudinal (■) and transverse (◆) velocities were taken from Fig. 3. Apparent activation energies for wave propagation determined by linear regression were −23.4 kJ/mol ($r = 0.9998$) and −19.5 kJ/mol ($r = 0.9910$) for longitudinal and transverse wave propagation, respectively.

Ca^{2+} waves are thought to be initiated by spontaneous localized release of Ca^{2+} from an overloaded SR (Fabiato, 1985, 1992; Stern et al., 1988; Ishide et al., 1992). The subsequent propagation of the Ca^{2+} wave is assumed to be caused by at least three processes: diffusion of Ca^{2+} to adjacent release sites, binding of Ca^{2+} to SR Ca^{2+} release channels, and induction of Ca^{2+} release from the SR (CICR). In turn, release of Ca^{2+} is followed by its resequestration into the SR, which directs the wave. The velocity of the wave front is thus determined by the kinetics and regulation of the SR Ca^{2+} release channel, the amount of Ca^{2+} released, the diffusion coefficient of Ca^{2+} in the cytosol and myofilament space, and the distribution of release sites (Fabiato, 1985, 1992; Stern et al., 1988; Wier and Blatter, 1991; Stern, 1992).

The major finding of this study is the anisotropy of wave propagation: Ca^{2+} waves move faster in the longitudinal than in the transverse direction in the myocyte. Taking into account that Ca^{2+} waves are accompanied by propagating contraction bands and that contraction is confined to the longitudinal direction, it might be argued that the observed anisotropy is an artifact resulting from anisotropic contraction. However, this is not the case: a contraction band involving 12–14 sarcomers leads to 3–5% cell shortening only. This contraction band lags behind the front of the Ca^{2+} wave by about 80 ms (Ishide et al., 1992; Williams et al., 1992). At the beginning of the Ca^{2+} wave when the contraction band is still developing, it may even pull the Ca^{2+} wavefront backwards and reduce the longitudinal velocity of the Ca^{2+} wave. Once the contraction band extends over 12–14 sarcomers, it moves at constant speed and width through the cell and should not have an influence on longitudinal wave velocity. Hence, anisotropic contraction is not the reason for the anisotropic propagation of Ca^{2+} waves.

We determined the temperature dependence of propagation velocites to identify the rate-limiting process in transverse and longitudinal wave spreading. Differences between longitudinal and transverse wave velocities were observed in the temperature range 17–37°C. The apparent activation energies for both processes derived from an Arrhenius plot of velocities (Fig. 5) were about −20 kJ/mol. This is a relatively low activation energy for a complex process such as wave propagation. When applied to a series of reactions, an Arrhenius plot reveals the temperature dependence of the velocity of the rate-limiting reaction step (Johnson et al., 1974). Wave propagation is thought to consist of repeated Ca^{2+} binding, release, and diffusion. The activation energies of wave propagation obtained by us are slightly larger than activation energies for diffusion of ions in aqueous solutions (−17 to −19 kJ/mol; Erdey-Grüz, 1974). This difference may be attributed to the higher viscosity of the cytosol as compared to an electrolyte. In contrast, gating of ionic channels involving conformational changes of the channel protein requires two- to threefold higher activation energies (Hille, 1984). In conclusion, the apparent activation energy for wave propagation of −20 kJ/mol is consistent with a diffusion-limited process.

Because activation energies were approximately the same for both longitudinal and transverse wave propagation, the observed anisotropy must have resulted from a structural microscopic anisotropy that exerts a direction-dependent influence on Ca^{2+} diffusion. In Fig. 6, the arrangement of myofilaments (*A*) and that of SR organization and diffusional spaces for Ca^{2+} (*B*) is shown schematically in a longitudinal section. Ca^{2+} release channels are confined to junctional and corbular SR that contain calsequestrin and store Ca^{2+} (Sommer and Jennings, 1983; Jorgensen et al., 1993). Junctional SR is located at the Z lines in close apposition to the t-tubules. There, Ca^{2+} influx through L-type Ca^{2+} channels induces CICR from the junctional SR in physiological excitation-contraction coupling. Corbular SR has no contact to the t-tubules but is located next to junctional SR within the I-band (Jorgensen et al., 1993) (Fig. 6). Its proposed physiological function is to amplify the Ca^{2+} released from junctional SR by CICR (Jorgensen et al. 1993). This assumption is supported by the finding that in rat myocytes the ratio between dihydropyridine receptors (L-type Ca^{2+} channels) in the sarcolemma and ryanodine receptors (SR Ca^{2+} release channels) is about 1:7 (Bers and Stiffel, 1993).

To assess the influence of the ultrastructural anisotropy on regenerative wave propagation, we consider the case of one-dimensional Ca^{2+} diffusion released from a plane, e.g., longitudinal Ca^{2+} diffusion from one Z disc to the next neglecting corbular SR. Between these release planes, no amplification of the Ca^{2+} signal occurs, and the peak Ca^{2+} value decreases inversely with the distance from the source. Assuming that release is triggered by a threshold concentration of Ca^{2+}, the overall velocity of a Ca^{2+} wave varies inversely with the distance between successive release regions. A larger distance between release regions in the transverse direction, d_t, than that in the longitudinal direction, d_l, would explain the observed anisotropy of wave propagation.

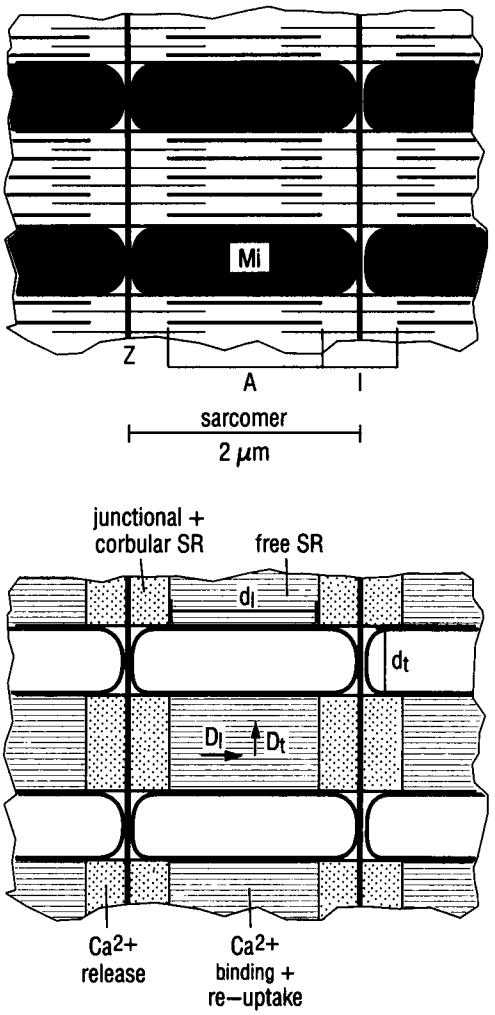

FIGURE 6 Model of sarcomere organization in a cardiomyocyte in a longitudinal section. (*A*) The arrangement of thin and thick filaments between Z lines, which form A and I bands. Myofilaments are periodically interrupted by parallel rows of mitochondria (Mi) in the transverse direction. (*B*) The topology of SR organization and of diffusion spaces for Ca^{2+} with regard to the scheme in *A*. Ca^{2+} is released from junctional SR at the Z lines and from corbular SR located within the I bands (*dotted* areas). It binds to the myofilaments and is finally resequestered by the network of free SR (*hatched* areas). For wave propagation, Ca^{2+} has to diffuse to the next release site where it can trigger CICR at sufficient concentration. In the longitudinal direction, Ca^{2+} ions have to overcome the critical distance d_l by diffusion before they will be amplified by CICR. In the transverse direction, the critical distance d_t has to be overcome. In addition, mitochondria act as diffusion barriers. Furthermore, diffusion in the myofilament space may be anisotropic because of the highly ordered arrangement of the myofilaments, i.e., direction-dependent diffusion coefficients D_l and D_t may exist.

Unfortunately, the exact arrangement and spacing of both junctional and corbular SR within release regions are not known. Longitudinally, a myocyte consists of identical subunits, the sarcomers, so d_l should be a constant, and an estimate for it is the width of an A band, i.e., 1.3 μm. In the transverse direction, myofibrils surrounded and wrapped by SR are interrupted by rows of mitochondria (Fig. 6 *A*) at an average distance of 0.6 μm (varying from 0.5 to 2 μm; Uehara et al., 1976; Sommer and Jennings, 1983). If Ca^{2+} release sites were homogeneously distributed over the whole I bands (*dotted* areas in Fig. 6 *B*) then d_t would be smaller than d_l. Thus, the spatial arrangement of regions containing Ca^{2+} release sites would favor transverse over longitudinal propagation. This is in contradiction to the experimental results. An explanation might be that Ca^{2+} release sites are clustered rather than homogeneously distributed within the I bands, thereby lengthening the critical distances d_t between release areas in transverse direction. Interestingly, a clustered arrangement of SR release channels has been proposed on a theoretical basis to explain graded release of Ca^{2+} from the SR in excitation-contraction coupling (Stern, 1992).

An alternative explanation of direction-dependent velocities takes into account the anisotropic arrangement of diffusion obstacles in a cardiomyocyte. Ca^{2+} ions diffusing in transverse direction periodically encounter rows of mitochondria (Fig. 6 *A*), which occupy as much as 32% of total cell volume (Barth et al., 1992). These mitochondria comprise large diffusion barriers (0.6 × 2 μm) and, therefore, lengthen the effective transverse distance from one release site to the next. Furthermore, the myofilaments themselves may act as diffusion obstacles. The marked anisotropic arrangement of the myofilaments suggests that they restrict diffusion in a direction-dependent manner. Taking into account that the myofilamental space occupies as much as 61% of total cell volume, whereas "free" cytosol amounts to 7% only (Barth et al., 1992), this effect might be significant.

Direction-dependent diffusion coefficients have been evaluated in a two-dimensional membrane model with alternating parallel stripes of fluid and solid lipid (Owicki and McConnell; 1980). Both transverse and longitudinal diffusion coefficients were smaller than that of the fluid phase. Lateral diffusion became "channeled" between the solid stripes, leading to a much larger reduction of the transverse diffusion coefficient than of the longitudinal one. This "channeling effect" probably also applies to diffusion in a three-dimensional system with cylindrical obstacles such as a cardiomyocyte. In contrast to the two-dimensional system, ions in the three-dimensional system may bypass the cylinders of low permeability rather than traversing them. In this case, however, their effective transverse velocity is reduced because of an increased path length. Taken together, it seems likely that diffusion of Ca^{2+} is channeled by the highly ordered myofilaments and by rows of mitochondria by facilitating the movement of Ca^{2+} in the longitudinal direction and restricting it in the transverse direction.

It is unknown whether cellular Ca^{2+} waves occur in situ in a normal heart. Hypotheses have been put forward that Ca^{2+} waves stochastically distributed over the whole heart control diastolic tension (Lakatta, 1992). As the frequency of Ca^{2+} wave occurrence in isolated cells rises with increasing Ca^{2+} load, waves may occur under pathological conditions, e.g., in ischemia or arrhythmia. A cellular Ca^{2+} wave propagating shortly before a regular excitation of the ventricular tissue will inhibit normal contraction of that cell because parts of SR are still refractory to CICR (Stern et al., 1988).

Anisotropic propagation of a Ca^{2+} wave combined with a localized refractory region will facilitate the occurrence of spiral waves, resembling the pathological conduction phenomenon of re-entry at the cellular level. Circulating spiral waves have recently been described using confocal ratiometric Ca^{2+} imaging in guinea pig cardiomyocytes (Lipp and Niggli, 1993). Our results indicate that these nonlinear waves are also present in rat myocytes. One can imagine that a circulating spiral wave will inhibit the normal functioning of a cell for a longer period of time. As Ca^{2+} waves are capable of jumping over to adjacent cells via gap junctions (Takamatsu et al., 1991; Engel et al., manuscript in preparation) a cell exhibiting spiral waves may also inhibit physiological functioning of its neighbors.

We wish to thank Silke Meyer for excellent technical assistance, Gunnar Krüger for his contribution in image processing, and Thomas Heimburg for stimulating discussions.

This work was supported by the Deutsche Forschungsgemeinschaft (SFB 330) and by the Association for International Cancer Research (U. K.).

REFERENCES

Barth, E., G. Stämmler, B. Speiser, and J. Schaper. 1992. Ultrastructural quantitation of mitochondria and myofilaments in cardiac muscle from 10 different animal species including man. *J. Mol. Cell. Cardiol.* 24:669–681.

Berlin, J. R., M. B. Cannell, and W. J. Lederer. 1988. Cellular origins of the transient inward current in cardiac myocytes. *Circ. Res.* 65:115–126.

Bers, D. M., and V. Stiffel. 1993. Ratio of ryanodine to dihydropyridine receptors in cardiac and skeletal muscle and implications for E-C coupling. *Am J. Physiol.* 264:C1587–C1593.

Erdey-Grüz, T. 1974. Transport phenomena in aqueous solutions. Adam Hilger, London. 194 pp.

Fabiato, A. 1985. Time and calcium dependence of activation and inactivation of calcium-induced release of calcium from the sarcoplasmic reticulum of a skinned canine cardiac Purkinje cell. *J. Gen. Physiol.* 85: 247–289.

Fabiato, A. 1992. Two kinds of calcium-induced release of calcium from the sarcoplasmic reticulum of skinned cardiac cells. *In* Excitation-Contraction Coupling in Skeletal, Cardiac and Smooth Muscle. G. B. Frank, editor. Plenum Press, New York. 245–262.

Fleischer, S., and M. Inui. 1989. Biochemistry and biophysics of excitation-contraction coupling. *Annu Rev. Biophys. Biophys. Chem.* 18:333–364.

Grouselle, M., B. Stuyvers, S. Bonoron-Adele, P. Besse, and D. Georges-cauld. 1991. Digital-imaging microscopy analysis of calcium release from sarcoplasmic reticulum in single rat cardiac myocytes. *Pflügers Arch.* 418:109–119.

Hille, B. 1984. Ionic channels of excitable membranes. Sinauer Associates Inc., Sunderland, MA. 49 pp.

Ishide, N., T. Urayama, K. I. Inoue, T. Komaru, and T. Takishima. 1990. Propagation and collision characteristics of calcium waves in rat myocytes. *Am. J. Physiol.* 259:H940-H950.

Ishide, N., M. Miura, M. Sakurai, and T. Takishima. 1992. Initiation and development of calcium waves in rat myocytes. *Am. J. Physiol.* 263: H327–H332.

Johnson, F. H., H. Eyring, and B. J. Stover. 1974. The theory of rate processes in biology and medicine. Wiley & Sons, New York. 169 pp.

Jorgensen, A. O., A. C. Y. Shen, W. Arnold, P. S. McPherson, and K. P. Campbell. 1993. The Ca^{2+} release channel/ryanodine receptor is localized in junctional and corbular sarcoplasmic reticulum in cardiac muscle. *J. Cell Biol.* 120:969–980.

Lakatta, E. 1992. Functional implications of spontaneous sarcoplasmic reticulum Ca^{2+} release in the heart. *Cardiovasc. Res.* 26:193–214.

Lipp, P., and E. Niggli. 1993. Microscopic spiral waves reveal positive feedback in subcellular calcium signaling. *Biophys. J.* 65:2272–2276.

Minta, A., J. P. Y. Kao, and R. Y. Tsien. 1989. Fluorescent indicators for cytosolic calcium based on rhodamine and fluorescein chromophores. *J. Biol. Chem.* 264:8171–817.

O'Rourke, B., D. K. Reibel, and A. P. Thomas. 1990. High-speed digital imaging of cytosolic Ca^{2+} and contraction in single cardiomyocytes. *Am. J. Physiol.* 259:H230–H242.

Owicki, J. C., and H. M. McConnell. 1980. Lateral diffusion in inhomogeneous membranes. *Biophys. J.* 30:383–398.

Piper, H. M., I. Probst, P. Schwartz, F. J. Huetter, and P. G. Spieckermann. 1982. Culturing of calcium stable adult rat cardiac myocytes. *J. Mol. Cell. Cardiol.* 14:397–412.

Rieser, G., R. Sabbadini, P. Paolini, M. Fry, and G. Inesi. 1979. Sarcomere motion in isolated cardiac cells. *Am. J. Physiol.* 236:C70–C77.

Sommer, J. R., and R. B. Jennings. 1986. Ultrastructure of cardiac muscle. *In* The Heart and Cardiovascular System. Vol. 1. H. A. Fozzard, E. Haber, R. B. Jennings, A. M. Katz, and H. E. Morgan, editors. Raven Press, New York. 61–100.

Stern, M. D., M. C. Capogrossi, and E. G. Lakatta. 1988. Spontaneous calcium release from the sarcoplasmic reticulum in myocardial cells: mechanisms and consequences. *Cell Calcium.* 9:247–256.

Stern, M. D. 1992. Theory of excitation-contraction coupling in cardiac muscle. *Biophys. J.* 63:497–517.

Takamatsu, T., and W. G. Wier. 1990. Calcium waves in mammalian heart: quantification of origin, magnitude, waveform, and velocity. *FASEB J.* 4:1519–1525.

Takamatsu, T., T. Minamikawa, H. Kawachi, and S. Fujita. 1991. Imaging of calcium wave propagation in guinea-pig ventricular cell pairs by confocal laser scanning microscopy. *Cell Struct. Funct.* 16:341–346.

Uehara, Y., G. R. Campbell, and G. Burnstock. 1976. Muscle and its innervation. Edward Arnold, London. 6 pp.

Wier, W. G., and L. A. Blatter. 1991. Ca^{2+}-oscillations and Ca^{2+}-waves in mammalian cardiac and vascular smooth muscle cells. *Cell Calcium.* 12:241–254.

Williams, D. A., L. M. Delbridge, S. H. Cody, P. J. Harris, and T. O. Morgan. 1992. Spontaneous and propagated calcium release in isolated cardiac myocytes viewed by confocal microscopy. *Am. J. Physiol.* 262:C731–C742.